Electrical Power and Energy Systems 119 (2020) 105885

Contents lists available at ScienceDirect

Electrical Power and Energy Systems

journal homepage: www.elsevier.com/locate/ijepes

Multi-objective optimal short-term planning of renewable distributed generations and capacitor banks in power system considering different uncertainties including plug-in electric vehicles

Saeed Zeynali, Naghi Rostami*, M.R Feyzi

Faculty of Electrical and Computer Engineering, University of Tabriz, Tabriz, Iran

ARTICLE INFO

Keywords:
Renewable distributed generation
Point estimate method
Sizing and siting
Multi-objective optimization
Chance constrained programming

ABSTRACT

The increasing penetration of solar distributed generations (SDGs) and wind distributed generations (WDGs) together with plug-in electric vehicles (PEVs) will lead to a promising amount of reduction in greenhouse gas emissions. Nevertheless, they bring about adversities such as uncertainty in production-load sides, augmented power loss, and voltage instability in the power system, which should be carefully addressed to increase the reliability. In this concern, this paper proposes a multi-objective optimization methodology for sizing and siting of SDGs, WDGs, and capacitor banks (CBs) in the power system considering uncertainties stemmed from PEVs load demand, solar irradiance, wind speed, and the conventional load. The understudy objectives are the voltage stability index, green-house gas emissions, and the total cost. An unconventional point estimate method (PEM) is used to handle the related uncertainties, and chance-constrained programming method is deployed to deal with smooth constraints. The corresponding probability distribution functions of output variables are estimated by the maximum entropy method. Furthermore, robustness analysis is made by Monte Carlo simulation (MCS). The proposed methodology is applied to a typical radial distribution network. The results show that the presence of PEV's significantly increases the load demand, which results in voltage collapse in the distribution system without the presence of distributed generations. However, the proposed probabilistic method ensures the safe operation of the distribution system with the optimal allocation of renewable distributed generations and CBs. Moreover, the results of deterministic and probabilistic cases are compared under different penetration levels of PEVs. The best tradeoff solution of the Pareto front is selected by the fuzzy satisfying method.

1. Introduction

The leading motivations in integrating distributed generations (DGs) in power systems are loss reduction, increasing reliability and voltage profile improvement [1]. However, the well-known defects of conventional DGs and the evident improvement in the competitiveness of renewable energy sources (RES) in terms of capital cost are encouraging investors to replace conventional DGs with solar distributed generations (SDGs) and wind distributed generations (WDGs) [2,3]. Optimal integration of these renewable DGs in power systems is crucial for their safe and economical operation [4]. Natural intermittencies of solar irradiation, wind speed, and plug-in electric vehicles (PEVs) load demand as a new aspect of power system should also be assimilated into sizing and siting problems, which is a mixed-integer nonlinear problem subjected to multiple objectives and constraints and many local optimums [5]. Additionally, the problem should handle these uncertainties with a reasonable tradeoff between computational burden and accuracy. Moreover, it might be in favor of the system operator to ignore the small probabilities of violation for soft constraints such as voltage and power limits [6].

According to the literature, DG planning can be generally categorized into single objective and multi-objective formulation [7]. They can also be categorized into subcategories such as deterministic, probabilistic, or in terms of the algorithm they apply, such as metaheuristic, analytical, etc. [5]. In the field of multi-objective DG allocation and sizing problems, some significant contributions have been made by [8–13]. In [8] a modified non-dominated sorting genetic algorithm is used to maximize the profit of distribution company and DG owners. Similarly, authors in [13] deploy a non-dominated sorting genetic algorithm for minimizing operation cost, planning cost and improving voltage profile in a tri-objective function. Reference [9] minimizes power loss and improves the voltages stability index by planning SDGs

* Corresponding author.
E-mail addresses: saeedzeynali96@ms.tabrizu.ac.ir (S. Zeynali), n-rostami@tabrizu.ac.ir (N. Rostami), feyzi@tabrizu.ac.ir (M.R. Feyzi).

https://doi.org/10.1016/j.ijepes.2020.105885
Received 27 August 2019; Received in revised form 8 January 2020; Accepted 27 January 2020

Nomenclature

Parameters

v	Wind speed (m/s)
$f_w(v)$	Weibull probability distribution function for wind speed
k,C	Shape and scale parameters of the Weibull probability distribution function (real)
ϕ	Solar irradiation (kW/m^2)
$f_B(\phi)$	Beta probability distribution function for solar irradiance
a, B	Shape parameters of beta probability distribution function (real)
v_{in} /v_{out} /v_r	Cut in/out/rated speed of wind turbine (m/s)
η	Efficiency of solar photovoltaic panels
T_{pv}	Ambient temperature (°C)
U	Set of random variables in standard normal space
X	Set of input random variables
$\pi_{\ell,Y}$	Probability of ℓth random variable and Yth point
P_i^D /Q_i^D	Active/reactive load demand in ith node
Ef	Per kW emission (kg/kW)
$V_{\min}/V_{\max}$	Minimum/Maximum allowable voltage value (v)
$\gamma_{V\max}/\gamma_{V\min}$	Probability of maximum/minimum allowable voltage Violation
$S^{\max}$	Maximum allowable power value (kVA)
$\gamma_{S\max}$	Probability of maximum line power violation
Ω	Feasible search space
ob	Number of objectives
F_1, F_2	Scaling factor
$\bar{N}$	Number of individuals in the archive
ρ	Selection pressure
$ICWDG$	Per kVA installation cost of wind distributed generation ($/kVA)
$ICSDG$	Per kVA installation cost of solar distributed generation ($/kVA)
a_1,a_2,a_3,a_4	Polynomial function coefficients for capacitor bank's cost
$WDG_{\max}$	Maximum allowable wind distributed generation capacity (kVA)
$CB_{\max}$	Maximum allowable capacitor bank capacity (kVAR)
$SDG_{\max}$	Maximum allowable solar distributed generation capacity (kVA)
Inf /Int	Inflation / interest rate (%)
P_i^{PEV}	Power demand of plug-in electric vehicle in ith bus (kW)
$\varphi_{\max}$	Maximum allowable voltage angle
T	Planning period (years)
T_s	Duration of the sth season (days)
C^{pr}	Active power price ($/kW)
$OMWDG$ / $OMSDG$	Operation and maintenance cost of wind/solar distributed generator ($/KW/day)
X_l /R_l	Line reactance/resistance (Ω)
Cr	Crossover rate
N_{var}	Number of decision variables

Variables

P^{WDG}/P^{SDG}	Output power of wind/solar distributed generator (kW)
x_i^{WDG}/ x_i^{SDG}	Size of wind/solar distributed generator (kVA)
S_{pv}	Area of the installed SDGs (m^2)
μ_ℓ	Mean value of output function considering only the ℓth random variable
μ_G	Mean value of output random variable
G^μ	The output of function when all random variables are set to their mean value
σ_ℓ	Standard deviation of output random variable considering only the ℓth variable
σ_G	Standard deviation of output random variable
$\alpha_{3\ell}$	Skewness of output random variable considering Only the ℓth variable
α_{3G}	Skewness of output random variable
$\alpha_{4\ell}$	Kurtosis of output random variable considering only the ℓth variable
α_{4G}	Kurtosis of output random variable
$p(X)$	Estimated probability distribution function of output random variable
λ_m	Lagrange multiplier
μ_n'	Non-central stochastic moments of output variable
f_1	Cost objective function
f_2	Voltage stability objective function
f_3	Emission objective function
IC	Installation cost ($)
OM	Operation and maintenance cost ($)
$CWDG^{ins}$	Installation cost of wind distributed generator ($)
$CSDG^{ins}$	Installation cost of the solar distributed generator ($)
x_i^{CB}	Size of capacitor banks (kVAR)
I_l	Line current (A)
V	Voltage value (pu)
P_i / Q_i	Absorbed active/reactive power in ith bus (kW/kVAR)
φ_i	Voltage angle in ith bus
P_i^{WDG}/P_i^{SDG}	Active power generated in ith bus by wind/solar distributed generation (kW)
Q_i^{CB}	Reactive power generated in ith bus by capacitor bank (kVAR)
$loss$	Active power loss (kW)
$loss^\mu$	Value of loss when all input RVs are set equal to their mean value (kW)
μ^{loss}	Mean value of active power loss (kW)
$CWDG^{OM}$ /$CSDG^{OM}$	Operation and maintenance cost of wind/solar distributed generator ($)
SI	Voltage stability index
V_s	Voltage value at sending end of the line (v)
P_r	Active power at receiving end of the line (kW)
Q_s	Reactive power at sending end of the line (kVAR)
μ^{SI_L}	Mean value of voltage stability index of Lth line
E	Emission (kg)
S_{sb}	Power absorbed from substation (kVA)
μ^E	Mean value of emission (kg) ***
E_μ	Emission value when all the variables are set to Their mean value (kg)***
V^{PDF}	probability distribution function of node voltage***
S^{PDF}	Probability distribution of of lines' power
x	Decision variable vector
$F(x)$	Objective function vector
x_1, x_2	A feasible solution vector
$s(h)$	Strength of hth solution
P_t	Main population
$\bar{P}_t$	Archive population
$D(h)$	Distance factor of the hth solution
$F(h)$	Fitness of the hth solution
σ_h^k	Distance of hth solution from its kth neighbor
$\overrightarrow{Z_h^g}$	Donor vector for hth offspring in gth generation
r_1^h, r_2^h, r_3^h, r_4^h	Dissimilar random vectors
$pb(h)$	Selection probability of hth solution
$u_{h,q}^g$	qth variable of the hth offspring in gth generation
$x_{i,q}^g$	qth variable of the hth parent in gth generation

Acronyms

PEV	Plug-in electric vehicle
WDG	Wind distributed generation

SDG	Solar distributed generation
DG	Distributed generation
RV	Random variable
CB	Capacitor bank
PDF	Probability distribution function
PLF	Probabilistic load flow
MCS	Monte Carlo simulation
GA-DE-SPEAII	hybrid genetic algorithm and differential evolution based multi-objective strength Pareto evolutionary algorithm

Indices

ℓ	Index of random variables for set of *NR*
Y	Index of points in point estimate method for set of *NP*
m	Index of statistical moment for set of *Nm*
y	Index of year for set of *T*
s	Index of season for set of 4 seasons
t	Index of hour for set of 24 h
i, j	Index of power system nodes for set of *Nb*
l	Index of power system lines for set of *Nb*-1
su	Index of substation for set of *Ns*
κ	Index of objectives in multi-objective problem for set of *ob*
h, e	Index of individual solutions for the multi-objective problem
q	Index of variables in an individual solution for the multi-objective problem
g	Index for generations in multi-objective problem

and WDGs with particle swarm optimization. The authors in [10,11] have proposed a multi-objective optimization problem that uses teaching–learning and backtracking search algorithms, respectively. A cuckoo search algorithm is used by [12] to improve voltage profile with two different voltage stability index and minimize power loss. However, the references [9–12] use the weighted summation method, which is not appropriate for discovering non-convex Pareto fronts [14].

All the above-mentioned multi-objective studies are deterministic, and uncertainties are not addressed. Evidently, uncertainties related to WDG and SDGs power have ineligible impacts on the optimal and safe operation of the distribution system [15]. Optimal DG planning has been investigated from the uncertainty point of view by [16–20]. In [16] a dynamic programming approach is deployed which optimizes three objectives, including cost, technical constraint dissatisfaction, and emission. However, only one probability distribution function (PDF) is assumed for each uncertain parameter, and the seasonality effect is ignored. Reference [17] evaluates the integration of WDGs by MCS with the objective of maximizing social welfare. Likewise, an MCS-based model is proposed by Abdelaziz *et al* [18], which uses parallel processing capabilities to deal with a huge computational burden of MCS. Reference [19] suggests Latin-hypercube sampling and Cholesky decomposition to deal with correlated random data. The problem, however, is that simulation-based models proposed by [16–19] incur a huge computational burden. In this concern, an affine arithmetic interval decision making method is proposed by [20], which provides robust optimal results. However, this is an approximate method which only considers the upper and lower bounds of the uncertain parameters, and PDFs are ignored.

In the field of optimal DG planning, very few of the literature has paid attention to uncertainties derived from PEVs, which are soon going to impose considerably high load demand on power systems [21]. In this regard [22] assumes that PEVs load demand follows a normal PDF and [23] proposes a triangular fuzzy membership function for PEVs load demand. However, these assumptions aren't legitimate. In [24], data provided from national household travel survey (NHTS) [25] have been used to extract uncertain load demand of PEVs by MCS. The used data include arrival-departure time, daily traveled miles and vehicle type data. Later the same authors applied this methodology into the planning of WDGs and capacitor banks (CBs) [26]. However, they propose a single-objective problem and the main drawback of this reference is using Hong's point estimate method (PEM) [27–29] to deal with uncertainties. This method obtains a few discreet evaluation points for each random variable (RV) by solving a system of non-linear equations wherein standard central moments are used. The main disadvantage of this method is its liability to provide negative evaluation points for positive RVs such as wind speed, solar irradiation, or in this particular case, the load demand of PEVs. In other words, the points provided by this method are likely to be outside of the domain which RVs are defined [30,31].

In order to address problems in [26] and benefit from computational advantages of PEM, this paper uses Zhao's PEM [30], which always provides points within the defined limits of RVs. Additionally, unlike Hong's PEM, the number of points can be easily increased to get higher accuracy [32]. Chance constrained programming is an effective method to deal with soft constraints, such as feeders' maximum power or node voltages. This method is based on calculating the violation probability of the probabilistic constraints. Therefore, it requires the PDFs of the output variables. In simulation-based methods, such as MCS, there is a large set of data associated with output variables. Therefore, building PDFs is quite easy with conventional curve fitting methods. However, the PEM only provides the probability moments of the output variables. To create the PDFs from the probability moment maximum entropy method is used in this study, which is proven to be more accurate than other methods such as Gram-Charlier expansion [33]. To the best of authors' knowledge, this method has not been used in the literature to deal with chance constraints in power system studies. As a result of transportation electrification, the PEVs are soon going impose a huge uncertain load on the power systems, which is properly modeled in this study. Deterministic and probabilistic case studies are investigated to prove the advantages of the probabilistic method. The multi-objective probabilistic sizing and siting problem is solved by a hybrid genetic algorithm and differential evolution based multi-objective strength Pareto evolutionary algorithm (GA-DE-SPEA), which uses differential evolution operators for continuous sizing variables and a particular permutation-based genetic algorithm for discrete variables which doesn't locate different planning components on the same node due to geographical and practical limitations. The major contributions of this study can be outlined as follows:

- PEV's load demand is integrated into multi-objective SDG, WDG and CB planning
- Zhao's PEM is incorporated into renewable DG allocation problem, and the results are compared with MCS
- Pareto optimal front is obtained considering different penetration levels of PEVs
- Chance constrained programming is integrated into PEM-based problem by maximum entropy method

The paper is organized as follows: Problem formulation is provided in section 2. The proposed methodology is introduced in section 3. Results are analyzed in section 4, and eventually, the conclusions are drawn in section 5.

2. Formulation

The decision variables of the sizing and sitting problem are the size

and location of the planning components in the distribution system. The major assumptions of the understudy problem are sated below.

- The understudy distribution system is assumed to be radial.
- The backward/forward sweep load flow method is used to solve load flow equations.
- The power factor of the loads is assumed to be constants.
- Separate PDFs are assumed for conventional load demand and PEV load demand of every node in the power system.
- The number of planning components is specified by the planner.

2.1. Uncertainty modeling

The understudy optimization problem is considered to be a probabilistic function with uncertain input parameters and uncertain output variables. The uncertain input parameters are PEVs load demand, conventional loads, solar irradiation and wind speed. While the uncertain output variables are feeders power flow and voltage values. In this section, the PDF of input variables are introduced, then it is explained how this probabilistic function is handled by Zhao's PEM to obtain the stochastic moments of the output variables. Eventually, the maximum entropy method is introduced to obtain the PDFs of the output variables from their corresponding stochastic moments.

2.1.1. Probability distribution functions

Normal PDF is used to model uncertainties of the commercial and residential load. Weibull PDF in (1) is deployed to model wind speed uncertainties while PDF of solar irradiance is modeled by beta distribution [34] shown in (2). Since wind speed and solar irradiance patterns are particularly different for each season, a different PDF is considered for each season and the related shape and scale parameters are calculated via the maximum likelihood method (MLM) using the historical data.

$$f_w(v) = \frac{k}{C}\left(\frac{v}{C}\right)^{k-1} \exp\left[-\left(\frac{v}{C}\right)^{k}\right] \tag{1}$$

$$f_B(\phi) = \frac{\Gamma(a+B)}{\Gamma(a)\Gamma(B)}\phi^{\alpha-1}(1-\phi)^{B-1} \tag{2}$$

After calculating the discrete evaluation points for wind speed and solar irradiance by the PEM the wind power and solar power are estimated via (3) and (4), respectively.

$$P^{WDG} = \begin{cases} 0 \; v \leqslant v_{in},\, v \geqslant v_{out} \\ \frac{v - v_{in}}{v_r - v_{in}} x^{WDG} \; v_{in} \leqslant v \leqslant v_r \\ x^{DG} \; v_r \leqslant v \leqslant v_{out} \end{cases} \tag{3}$$

$$P^{SDG} = \eta S_{pv} \phi (1 - 0.005(T_{pv} - 25)) \tag{4}$$

Further explanation over the stochastic load demand of plug-in electric vehicles in the residential distribution network is provided in the methodology section.

2.1.1.1. Zhao's point estimate method (PEM). To calculate the expected value of objective functions, the PDF of voltage, and power values, probabilistic load flow (PLF) analysis should be carried out by taking all input RVs into account. In this study, Zhao's point estimate method is deployed to fulfill PLF [31] since it is proven to be computationally effective with a considerably high degree of accuracy in PLF analysis [30,32]. In this method, the number of points can be increased to get more accurate results.

First, by solving Hermite integration, the corresponding points and weights are obtained in the standard normal space. Then, using Rosenblatt transformation shown in Eqs. (5) and (6), the points are transformed into input RVs space. Considering the fact that standard normal space is defined over the domain of (-∞, +∞), any obtained point is undoubtedly feasible. Eventually, the conventional load flow equations denoted by G(X) is applied to these discrete states.

$$U = T(X) \tag{5}$$

$$X = T^{-1}(U) \tag{6}$$

Since input RVs are uncorrelated in standard normal space, the mean, the variance, the skewness, and the kurtosis of the output variable is estimated as follows. Further information and comprehensive examples about Zhao's PEM can be found in [31].

$$\mu_G = \sum_{\ell=1}^{NR} (\mu_\ell - G^\mu) + G^\mu \tag{7}$$

$$\sigma_G^2 = \sum_{\ell=1}^{NR} {\sigma_\ell}^2 \tag{8}$$

$$\alpha_{3G} = \frac{1}{{\sigma_G}^3} \sum_{\ell=1}^{NR} \alpha_{3\ell} \sigma_{\ell=1}^3 \tag{9}$$

$$\alpha_{4G} = \frac{1}{\sigma_G^4}\left(\sum_{\ell=1}^{NR} \alpha_{4\ell}\sigma_\ell^4 + 6\sum_{\ell=1}^{NR-1}\sum_{J>1}^{NR} \sigma_\ell^2 \sigma_J^2\right) \tag{10}$$

In this paper, the input data are assumed to be uncorrelated. However, the proposed method is capable of handling any possible correlation by Nataf transformation [35].

2.1.1.2. Maximum entropy (ME) method. The Maximum Entropy (ME) method [33] is utilized to rebuild the PDF of output RVs after obtaining the stochastic moments by PEM, as mentioned above. The PDF of output RVs is estimated by $p(X)$ shown in (11). The corresponding parameters of this function are calculated by solving the system of nonlinear equations demonstrated in (12). The probability distribution functions are used to calculate constraint violation probabilities, which is necessary in chance-constrained programming.

$$p(X) = exp\left[-\sum_{m=0}^{Nm} \lambda_m X^m\right] \tag{11}$$

$$\int_{-\infty}^{+\infty} X^n exp\left[-\sum_{m=0}^{Nm} \lambda_m X^m\right] = \mu_n' \quad n = 1,\ 2,\ ...,Nm \tag{12}$$

2.2. Objective functions

The multi-objective optimal SDG, WDG, and CB integration problems comprise three objectives, which are total cost, voltage stability index, and greenhouse gas emissions. The optimal value of decision variables should be determined subject to certain constraints. The expected values of the objective functions are calculated according to (7).

2.2.0.1. Cost objective function

Cost objective function consists of installation, operation, and maintenance cost of the SDGs, WDGs, and CBs during the planning period as follows:

$$Min.\, f_1 = IC + OM \tag{13}$$

The installation cost of CBs varies in a wide range depending on their capacity. Therefore, in this study, the installation cost of CBs is calculated by fitting a polynomial curve to available price data, as shown in (17). The total installation cost is calculated as follows:

$$IC = \sum_{i=1}^{Nb} [CWDG_i^{Ins}(x_i^{WDG}) + CCB_i^{Ins}(x_i^{CB}) + CSDG_i^{Ins}(x_i^{SDG})] \tag{14}$$

$$CWDG_i^{Ins}(x_i^{WDG}) = x_i^{WDG} \times ICWDG \qquad \forall \; 0 < x_i^{WDG} < WDG_{\max} \tag{15}$$

$$CSDG_i^{Ins}(x_i^{SDG}) = x_i^{SDG} \times ICSDG \quad \forall \ 0 < x_i^{SDG} < SDG_{\max} \tag{16}$$

$$CCB_i^{Ins}(x_i^{CB}) = a_4[x_i^{CB}]^4 + a_3[x_i^{CB}]^3 + a_2[x_i^{CB}]^2 + a_1[x_i^{CB}] \quad \forall \ 0 < x_i^{CB} < CB_{\max} \tag{17}$$

The expected value of power loss and the total operation cost during the planning period are calculated by (18)-(22)

$$loss = \sum_{l=1}^{Nl} R_l \times |I_l|^2 \tag{18}$$

$$\mu^{loss} = \sum_{\ell=1}^{NR}\left(\sum_{Y=1}^{NP}(\pi_{\ell,Y} \times loss_{\ell,Y}[T^{-1}(U_{\ell,Y})]) - loss^{\mu}\right) + loss^{\mu} \tag{19}$$

$$OM = \sum_{y=1}^{T}\sum_{s=1}^{4}\sum_{t=1}^{24} T_s \times (C_{s,t}^{pr} \times \mu_{s,t}^{loss} + \mathrm{CWDG}_{s,t}^{OM} + \mathrm{CSDG}_{s,t}^{OM}) \times \left(\frac{1+Inf}{1+Int}\right)^{y-1} \tag{20}$$

$$\mathrm{CWDG}^{OM} = \sum_{i=1}^{Nb} OMWDG \times x_i^{WDG} \tag{21}$$

$$\mathrm{CSDG}^{OM} = \sum_{i=1}^{Nb} OMSDG \times x_i^{SDG} \tag{22}$$

2.2.0.2. Voltage stability function

The voltage stability index (SI) proposed by [36] for radial distribution systems shown by (23) is used to determine the nodes which are more prone to voltage instability. The mean value of the voltage stability index is calculated by (24). Afterward, the second objective function is established by (25).

$$SI_l = |V_s|^4 - [4(P_rX_l - Q_sR_l)^2 - 4(P_rR_l - Q_sX_l)^2]|V_s|^2 \quad l = 1, 2, ...,Nl \tag{23}$$

$$\mu^{SIl} = \sum_{\ell=1}^{NR}\left(\sum_{Y=1}^{NP}\pi_{\ell,Y} \times SI_{l,\ell,Y}[T^{-1}(U_{\ell,Y})] - SI_l^{\mu}\right) + SI_l^{\mu} \quad l = 1, 2, ...,Nl \tag{24}$$

$$Max.\ f_2 = \sum_{y=1}^{Y}\sum_{s=1}^{4}\sum_{t=1}^{24} Min_l(\mu_{y,s,t}^{SI_l}) \tag{25}$$

2.2.0.3. Emission function

Considering emission as a function of the real power imported from the upstream power grid, it can be defined as shown in (26). The mean value of the emission is calculated by (27), and the third objective function is defined as (28). It should be emphasized that the real value of S_Q^{sb} will be positive when the power is absorbed from the upstream grid.

$$E = \sum_{su=1}^{Ns} Ef \times Max(real(S_{su}^{sb}), 0) \tag{26}$$

$$\mu^E = \sum_{\ell=1}^{NR}\left(\sum_{Y=1}^{NP}\pi_{\ell,Y} \times E_{\ell,Y}[T^{-1}(U_{\ell,Y})] - E_{\mu}\right) + E_{\mu} \tag{27}$$

$$Min.\ f_3 = \sum_{y=1}^{Y}\sum_{s=1}^{4}\sum_{t=1}^{24}\mu_{y,s,t}^{E} \tag{28}$$

2.3. Constraints

Equality and inequality constraints are inevitable parts of the most optimization problems, and the one represented in this paper is not an exception. On account of the probabilistic nature of the problem, the chance-constrained programming method is deemed to be suitable to deal with smooth variables' violations such as voltage values and power flow of the lines [37,38]. Chance-constrained programming is a method for dealing with probabilistic constraints. Instead of enforcing the constraints for every possible scenario, the probability of constraint violation is limited. For instance, in this study, the probability of violation for voltage values and feeders' nominal power is restricted to be less than 0.05. The probability of constraints violation is calculated by the PDFs of these variables, which are obtained from the previously explained maximum entropy method. In most cases, the operator is willing to endure small probabilities of constraint violation to achieve a possibly higher degree of optimality [39]. The chance constraints are stated by (29)–(30). The security constraints stated by (31)–(36) should be satisfied in any possible case.

$$p(V_{y,s,t,i}^{PDF}(X, x_i^{SDG}, x_i^{CB}, x_i^{WDG}) \geqslant V_{\min}) \geqslant \gamma_{V\min},\ p(V_{y,s,t,i}^{PDF}(X, x_i^{SDG}, x_i^{CB}, x_i^{WDG}) \leqslant V_{\max}) \geqslant \gamma_{V\max} \tag{29}$$

$$y = 1, 2, \cdots Ys = 1, 2, 3, 4t = 1, 2, \cdots 24i = 1, 2, \cdots, Nb$$

$$p(S_{l,y,s,t}^{PDF}(X, x_i^{SDG}, x_i^{CB}, x_i^{WDG}) \leq S_l^{\max}) \geq \gamma_{S\max} y = 1, 2, \cdots 4s = 1, 2, 3, 4t = 1, 2, \cdots 24 \tag{30}$$

$$\sum_{i=1}^{Nb} P_i^D + \sum_{i=1}^{Nb} P_i^{PEV} + \sum_{l=1}^{Nl} R_l \times |I_l|^2 = \sum_{i=1}^{Nb} P_i^{WDG} + \sum_{i=1}^{Nb} P_i^{SDG} \quad \textbf{R2. Q3} \tag{31}$$

$$\sum_{i=1}^{Nb} Q_i^D + \sum_{l=1}^{Nl} X_l \times |I_l|^2 = \sum_{i=1}^{Nb} Q_i^{CB} \quad \textbf{R2. Q3} \tag{32}$$

$$0 \leqslant P_i^{WDG} \leqslant x_i^{SDG} \quad i = 1, 2, ...,Nb \tag{33}$$

$$0 \leqslant P_i^{SDG} \leqslant x_i^{SDG} \quad i = 1, 2, ...,Nb \tag{34}$$

$$0 \leqslant Q_i^{CB} \leqslant x_i^{CB} \quad i = 1, 2, ...,Nb \tag{35}$$

$$-\varphi_{\max} \leqslant \varphi_i \leqslant \varphi_{\max} \quad i = 1, 2, ...,Nb \tag{36}$$

3. Methodology

3.1. Stochastic load demand of PEVs

Various uncertain parameters such as home arrival/departure time, driving patterns, daily traveled miles, vehicle type, etc. are involved in hourly stochastic load demand of PEVs. A practical method is proposed by [24], which takes all the uncertainties mentioned above into account, and calculates the hourly stochastic load demand using MCS. In this paper, the same method is deployed to extract the probability distribution of PEVs power demand, and it is considered to be active power. The probability distribution of input data such as daily traveled miles and arrival-departure time is demonstrated in Fig. 1, which are obtained from [40]. The hourly stochastic load demand for PEVs is demonstrated in Fig. 2 by violin plots. The inverse cumulative distribution function of PEVs load demand which is essential in Zhao's PEM is obtained by curve fitting methods to obtained samples from MCS

3.2. Streng Pareto evolutionary algorithm II (SPEA-II)

Almost all multi-objective evolutionary algorithms estimate optimal Pareto front of randomly created first population. Afterward, they mix individuals to develop possibly better Pareto members using algorithm-specific operators [41]. In general, Multi-objective optimization problems are defined as (37). A feasible solution such as x_1 dominates x_2

when (38) is satisfied [16]. The set of non-dominated solutions form the Pareto front.

$$F(x) = (f_1(x), \ldots, f_{ob}(x))^T \tag{37}$$

$$\text{s.t } x \in \Omega$$

$$\forall\, \varkappa \in \{1, \ldots, ob\} f_\varkappa(x_1) \leqslant f_\varkappa(x_2) \wedge \exists\, \varkappa \in \{1, \ldots, ob\} f_\varkappa(x_1) < f_\varkappa(x_2) \tag{38}$$

The authentic truncation and fitness assignment strategy of the SPEA-II algorithm [42] provides an in-depth insight into the density of the solutions on the Pareto front. Similar to most multi-objective evolutionary algorithms, an iteratively created population ($\bar{P}_t$) and for the best solutions ever found an archive population ($\bar{P}_t$) is proposed. Every single solution is characterized by strength, raw fitness, density and fitness which are obtained according to (39)–(42), respectively.

$$s(h) = \{e \mid e \in P_t + \bar{P}_t \wedge h \succ e\} \tag{39}$$

$$R(h) = \sum_{e \succ i} s(e)\ e \in P_t + \bar{P}_t \tag{40}$$

$$D(h) = \frac{1}{\sigma_h^k + 2} \tag{41}$$

$$F(h) = R(h) + D(h) \tag{42}$$

Non-dominated solutions have zero raw fitness. The archive population in multi-objective problems with numerous objectives is usually filled quickly with non-dominated solutions [43]. Hence, there should be a second evaluation reference to classify non-dominated individuals. In this concern, the density of the solutions is exploited [44], which is obtained from the standard Euclidean distance of individuals from one another. The distance to kth nearest neighbor of each individual is used to define the density factor which is 0.5 for the worst possible scenario. On account of the fact that the Pareto solutions possess a raw fitness value of zero, the best-dominated solutions will still have a higher fitness value than the worst non-dominated solution. This fitness assignment technique is used to truncate solutions when the archive is full. In this case, the dominated solutions will be first to get omitted. Subsequently, the non-dominated solutions positioned in denser areas will be omitted. Binary tournament selection and genetic algorithm are used in the SPEA-II algorithm. In this paper, slight modifications are made to parent selection. A hybrid GA-DE is incorporated to make the algorithm more suitable for sizing and siting problems [21]. Further explanation about the proposed algorithm is provided in the next section.

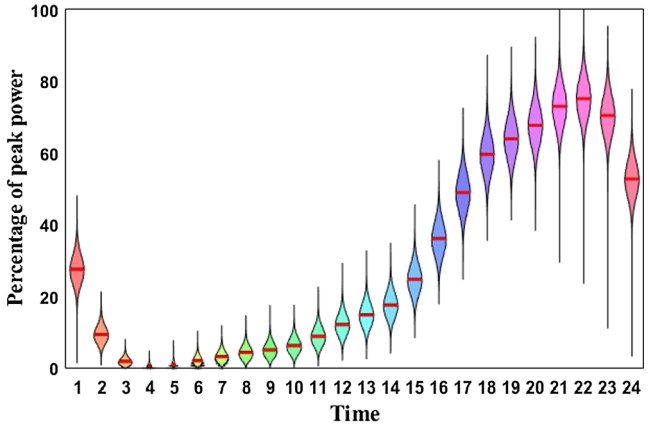

Fig. 2. PEVs hourly power demand distribution in violin plots.

3.3. Hybrid genetic algorithm and differential evolution based multi-objective strength Pareto evolutionary algorithm (GA-DE-SPEAII)

In general, the differential evolution algorithm deploys mutation and crossover operators to create an offspring for each parent solution [45]. The offspring replaces the parent if it is a more fit solution. Otherwise, the parent solution is kept intact. By iteratively repeating this process, the entire population is evolved toward the optimum solution. The mutation operator perturbs a set of randomly chosen vectors to create a different vector, which is also referred as the donor vector. Eventually, the crossover is used to create an offspring solution [46]. In this paper, all of the three well-known mutation strategies [47] demonstrated by (43)-(45) are used to benefit from their unique exploration and exploitation characteristics. The crossover method is chosen randomly by the algorithm.

$$\vec{Z}_h^g = \vec{x}_{r_1^h}^g + F_1.(\vec{x}_{r_2^h}^g - \vec{x}_{r_3^h}^g) \tag{43}$$

$$\vec{Z}_h^g = \vec{x}_h^g + F_2.(\vec{x}_{best}^g - \vec{x}_h^g) + F_2.(\vec{x}_{r_1^h}^g - \vec{x}_{r_2^h}^g) \tag{44}$$

$$\vec{Z}_h^g = \vec{x}_{best}^g + F_2.(\vec{x}_{r_1^h}^g - \vec{x}_{r_2^h}^g) + F_2.(\vec{x}_{r_3^h}^g - \vec{x}_{r_4^h}^g) \tag{45}$$

In a single objective optimization problem x_{best}^g can be defined as the best solution [48]. However, in a multi-objective problem, all the solutions on the Pareto front are a fit individual. In this regard, the roulette wheel selection method [49] is used with selection probabilities defined as follows:

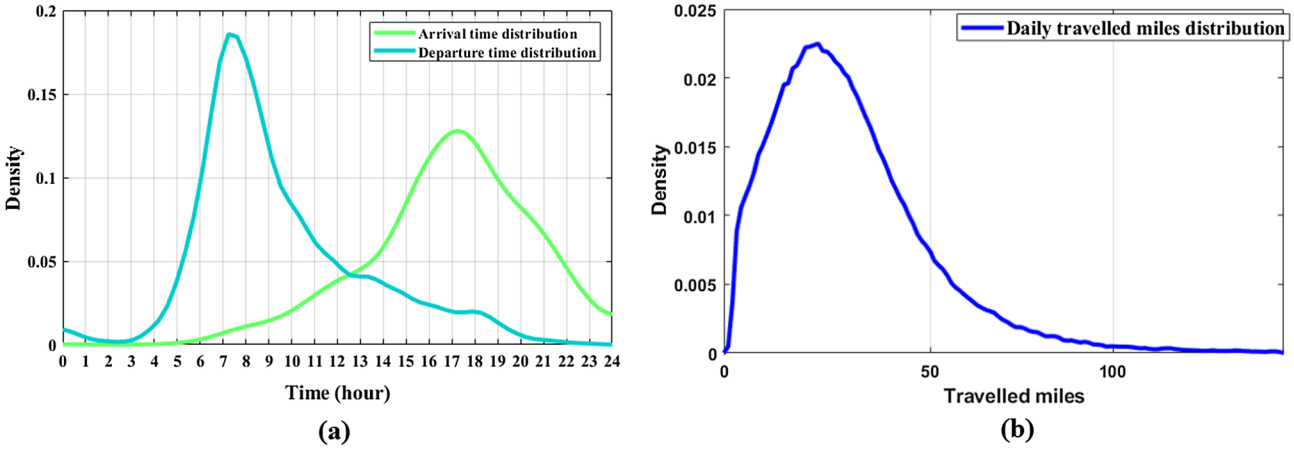

Fig. 1. The PDF of the stochastic data of PEVs according to NHTS data; (a) probability distribution of home arrival-departure time (b) probability distribution of daily travelled miles [40]

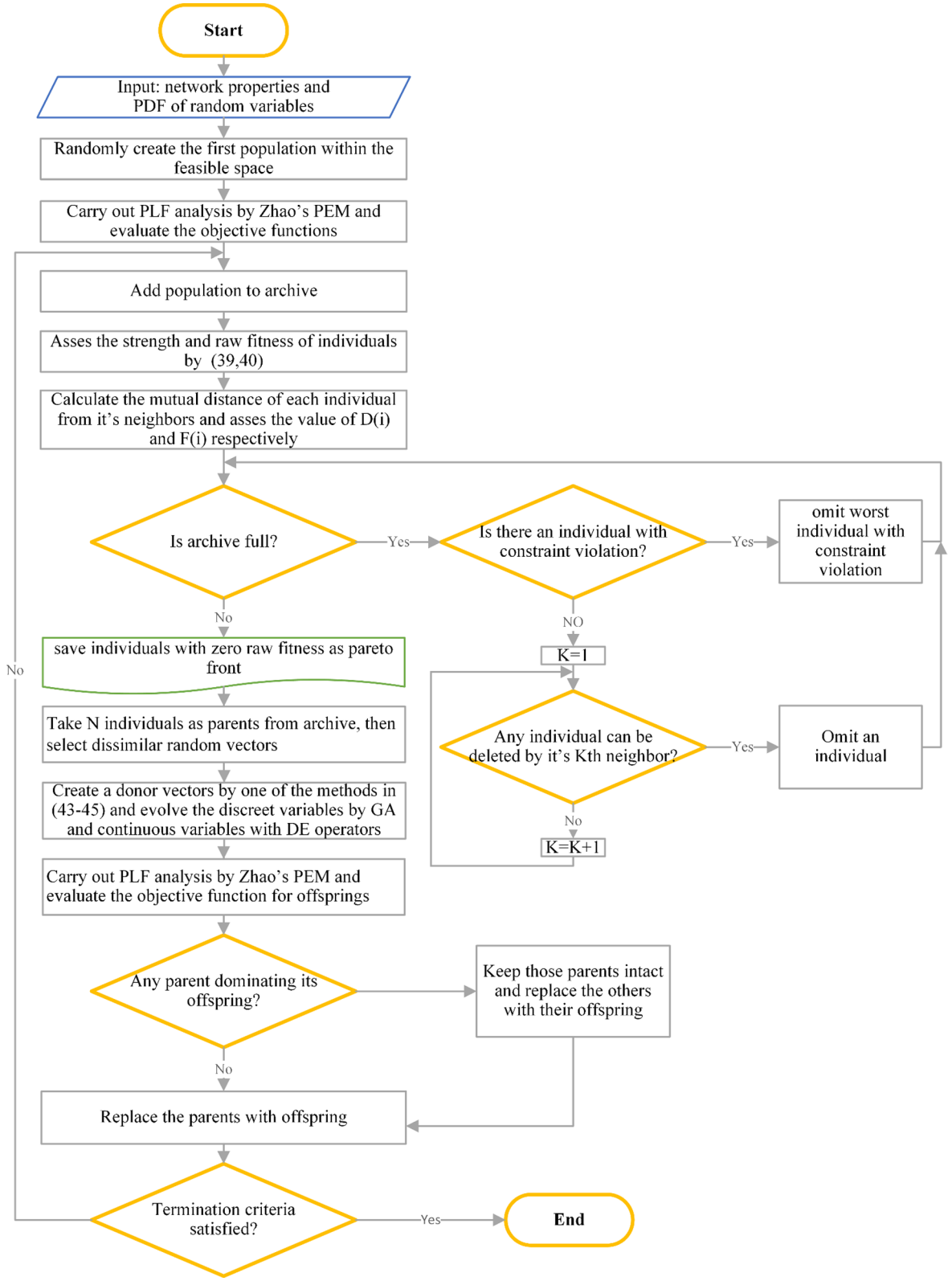

Fig. 3. Flowchart of the proposed GA-DE-SPEAII algorithm.

$$pb(h)_{archive} = \frac{\exp(-\rho \times F(h))}{\sum_{i=1}^{\bar{N}} \exp(-\rho \times F(h))} \tag{46}$$

This method increases the chance of mating for individuals with better fitness value. By adjusting the value of $\rho$the degree of elitism in the algorithm can be controlled. To get an offspring from a parent, the crossover should be applied as follows [50]:

$$u_{h,q}^{g} = \begin{Bmatrix} Z_{h,q}^{g} \; rand[0,\,1] \leqslant Cr \vee q = randi[1,\,N_{\text{var}}] \\ x_{h,q}^{g} \; \text{Otherwise} \end{Bmatrix} \tag{47}$$

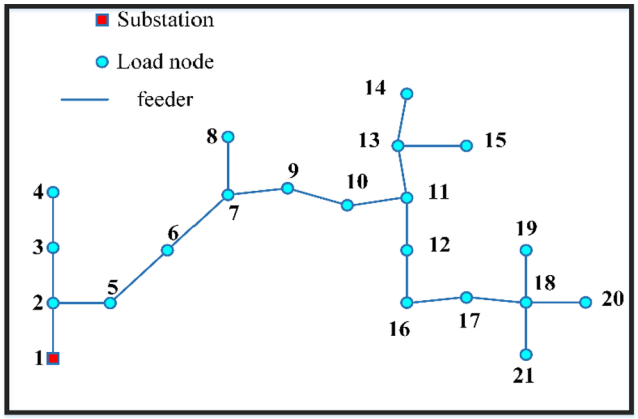

Fig. 4. The understudy 21-node system [53]

In sizing and siting problems, due to both geographical and technical limits SDGs, WDGs and CBs cannot be sited in the same node of the power system, which imposes a challenging constraint on the problem. In other words, none of the discreet siting variables should have the same values. The solution to this permutation-based problem is similar to the well-known Travelling salesman problem. Using a modified crossover and mutation operators [51,52] in GA, any obtained solution will satisfy the aforementioned constraint, which also reduces the search space of siting variables. The same method is applied in this paper, and the overall flowchart of the proposed GA-DE-SPEA algorithm is demonstrated by Fig. 3.

4. Results

The proposed algorithm is applied to a 21-node radial distribution network shown in Fig. 4, which is adopted from [53]. HV/MV substation is located at node 1, which connects the system to the upstream network. All nodes are deemed to be a legitimate installation site for any of the planning components. The residential loads and PEVs load demand are assumed to be located at nodes 2–16, and the commercial loads are located at nodes 17–21. The related electricity price and planning data are respectively summarized in Tables 1 and 2. The Weibull PDF of wind speed in each season and the PDF of solar irradiance in boxplot is illustrated in Figs. 5 and 6, respectively. The mean value of residential, and commercial loads' seasonal profiles for the understudy power system is plotted in Fig. 7.

The controller parameters of the algorithm, which are obtained by running the deterministic case for a few times with different settings are summarized in Table 3. The optimal Pareto front without any illegitimate constraint-violating individuals for the main scenario, which embodies 50% PEV penetration level is illustrated by Fig. 8

Obviously, on two-dimensional papers, it isn't feasible to demonstrate all the aspects of three-dimensional Pareto front. Therefore, it is a common act to plot two-dimensional projections [54], such as cost versus voltage stability or cost versus emission, which is demonstrated in Fig. 9, considering different penetration levels of PEVs. It should be noted that the dominance of the individuals should be evaluated by taking all the projections into account. The desirable Pareto front contains uniformly distributed individuals. In other words, they should be neatly scattered over the Pareto front. Nevertheless, the extremely constrained nature of this optimization problem makes some solutions infeasible, which should be omitted. To select the best trade-off solution, the Fuzzy satisfying method [16] is deployed in this study. The obtained results for the probabilistic case are demonstrated in Table 4, and for the deterministic case are demonstrated in Table 5. The increment in penetration levels of PEVs increases load demand, and accordingly, the total cost gets increased, the voltage stability index gets decreased, and emission gets increased. Therefore, the Pareto front gets shifted to worse areas of the objective space.

The probabilistic case consists of 37 RVs, which are namely, 15 RVs related to residential load, 5 RVs related to commercial loads, 15 RVs related to PEVs load demand at residential nodes, and 2 RVs for wind speed and solar irradiation, respectively. In this study, the 7-point scheme is deployed, which needs seven evaluations per RV. Consequently, 37 × 7 assessments are carried out for every single hour of the four seasons. Eventually, the power flow equation is solved 24,864 times per objective function evaluation, while the simulation-based methods require a considerably large amount of assessments per hour for a problem of this size [55]. The deterministic case needs only one power flow problem for every hour, wherein all input RVs are set equal to their expected values. In other words, the planning is performed only for a snapshot of the power system. From obtained results in Tables 4 and 5, it can be seen that in the deterministic case,

Table 1
Average electricity price for each season.

Average electricity price ($/MWh)				
	Spring	Summer	Autumn	Winter
Light load	95	95	82	82
Normal load	135	135	120	120
Peak load	160	160	140	140

Table 2
Parameters of the understudy system.

Parameter	Value
Wind turbine installation cost ($/MVA)	1,300,000
Wind turbine O&M cost ($/MVA/year)	5110
Solar PV installation cost ($/MVA)	1,000,000
Solar PV O&M cost ($/MVA/year)	9897
$\gamma_{V\min}$, $\gamma_{V\max}$, $\gamma_{S\max}$	0.95
Maximum allowed voltage deviation	0.05
Duration of the projects (year)	10
Power factor of the residential loads	0.981(lag)
Power factor of the commercial loads	0.911(lag)
Resistance of feeders (Ω/km)	0.2006
Reactance of feeders (Ω/km)	0.4026
Interest rate (%)	2.5
Inflation rate (%)	1.9
Polynomial coefficients of capacitor bank installation cost function	$a_1 = 16.23$, $a_2 = -0.1593$ $a_3 = 6.8e-4$, $a_4 = -1.048e-6$
Carbon emission (kg/kwh)	0.55428

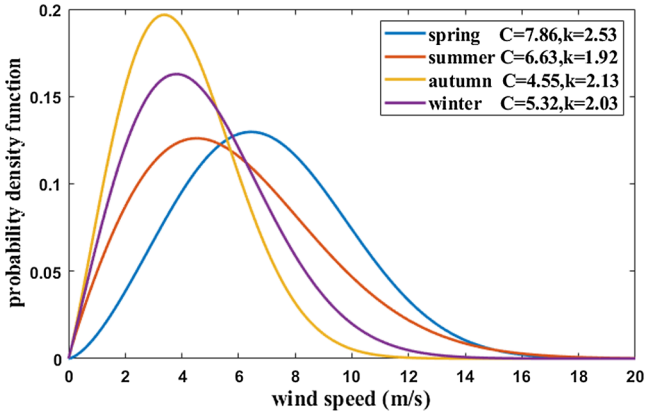

Fig. 5. Wind speed PDFs for each season.

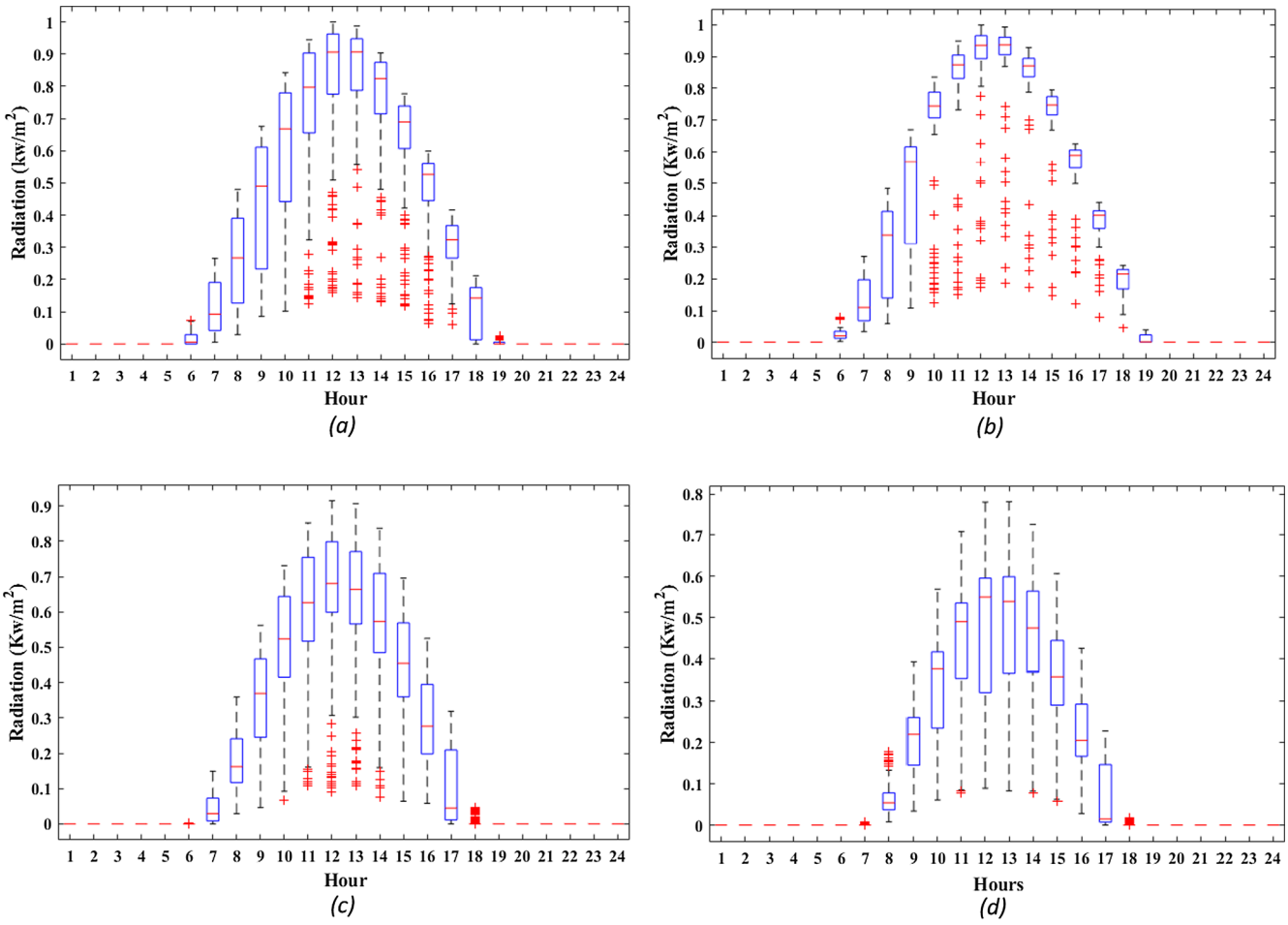

Fig. 6. PDF of solar irradiation; (a) spring (b) summer (c) autumn (d) winter.

Table 3
controller parameters of GA-DE-SPEAII.

Controller parameters	value
F_1	0.73
F_2	0.42
Cr	0.36
$\bar{N}$	600
Population size	200
Crossover type of GA	M−point
Mutation type of GA	Swapping [51]

components' locations are closer to the end nodes, which is in accordance with the results reported in the majority of the literature [56,57]. Since the end nodes suffer from lower voltage values, they need the planning components to be supported. On the other hand, in the probabilistic case, the components are distributed along the system. In the real-world conditions, the deterministic case will most probably impose severe damages upon the power system, and total blackout will be inevitable. For instance, the results obtained from the deterministic and probabilistic cases are applied to the power system, and the PDF of the voltage values are obtained by MCS. Fig. 10 demonstrates the PDF of voltage value at node 15 (the node with the lowest mean value of

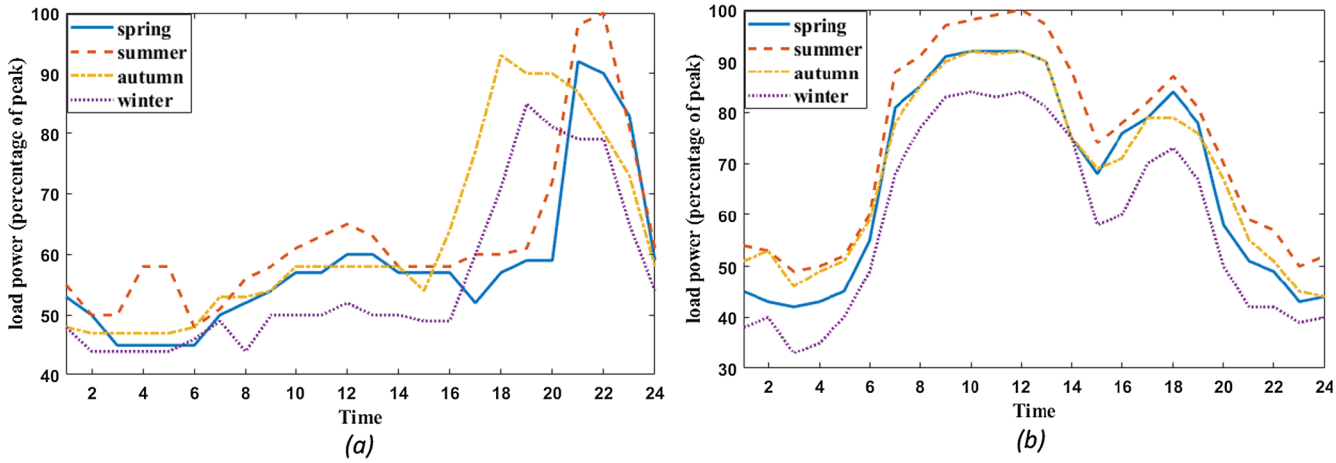

Fig. 7. Mean value of load power profile in each season, (a) residential, (b) commercial.

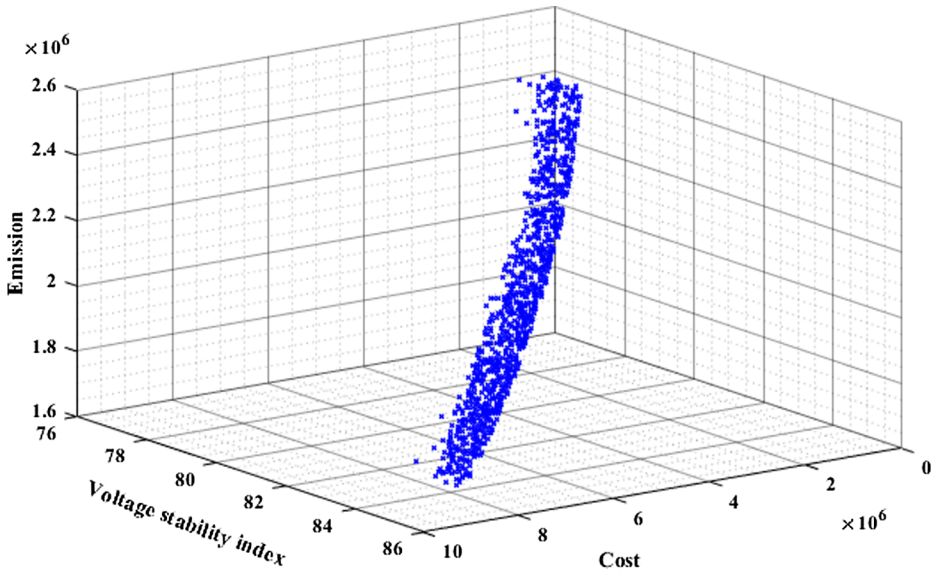

Fig. 8. Three-dimensional Pareto optimal front of multi-objective sizing and sitting problem.

voltage) and at hour 22 of spring. As can be seen, in the deterministic case, the probability of minimum voltage violation is unacceptably beyond the specified chance constraint probability. In the probabilistic case, however, the probability of violation is insignificantly small, which stems from estimation errors inherent in PEM and maximum-entropy method. As can be seen from Tables 4 and 5, the increments in penetration level of PEVs result in a higher capacity of the planning components since PEVs impose an extra load, which results in lower voltage stability, higher const, and higher emission. Therefore, more DG units should be installed to support the system. Moreover, the increments in PEV's penetration nonlinearly augments the optimal size of the planning equipment. In the probabilistic case, the location of the components is closer to the substation, which might not seem to be optimal. Whereas the system is more robust, and the probability of violation is very low. Another notable difference in the results of Tables 4 and 5 is that in the probabilistic case, the capacity of the planning components is considerably more than the deterministic case since the probabilistic case should provide valid results for a wide range of

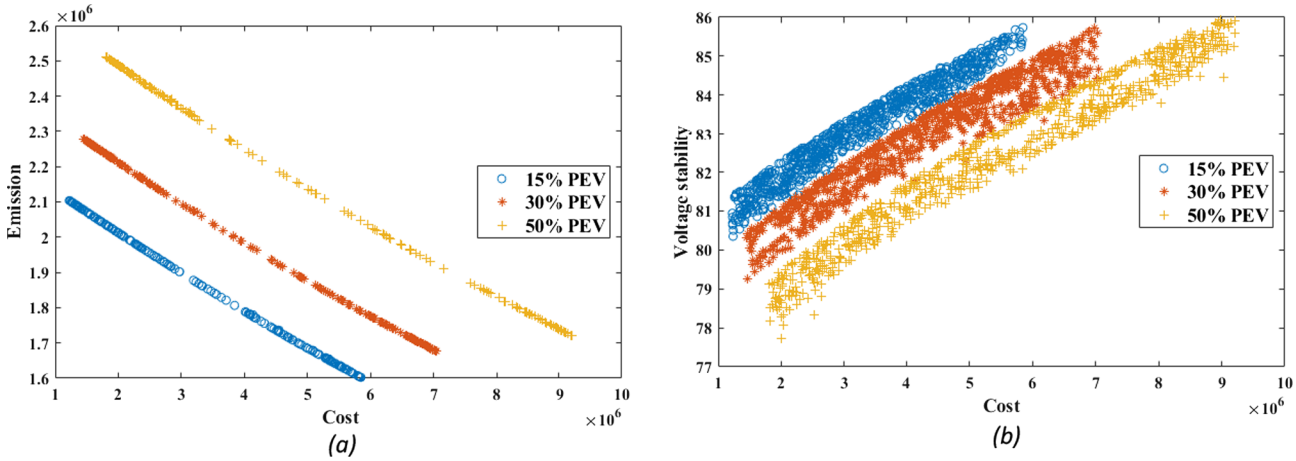

Fig. 9. Pareto front projections for different PEV penetration levels, (a) Cost VS Emission (b) Cost VS Voltage-stability.

Table 4
The results of the best trade-off solution for different PEV penetration in the probabilistic case.

PEV Penetration level %	Wind distributed generation (kVA)		Solar distributed generation (kVA)		Capacitor Bank (kVAR)	
	Location	Capacity	Location	Capacity	Location	Capacity
0	16	723	11	700	19	250
	18	956	–	–	20	175
15	13	412	20	995	15	220
	18	1255	–	–	17	255
30	15	1370	11	999	14	278
	18	620	16	480	20	294
50	13	1400	10	1000	8	298
	17	690	12	997	16	249
	–	–	–	–	20	300

Table 5
The results of the best trade-off solution for different PEV penetration in the deterministic case.

PEV Penetration level %	Wind distributed generation (kVA)		Solar distributed generation (kVA)		Capacitor Bank (kVAR)	
	Location	Capacity	Location	Capacity	Location	Capacity
0	19	829	18	255	16	195
	20	263	–	–	17	202
15	19	1105	18	395	11	255
	20	150	–	–	17	291
30	14	199	18	350	15	284
	17	720	20	417	16	290
50	17	1210	13	300	9	290
	18	780	19	695	16	260
	–	–	–	–	20	300

possible outcomes without violating the security constraints. As a result of using the proposed algorithm, none of the components are located on the same nodes. Three-dimensional boxplots in Fig. 11 illustrates the PDF of voltage at each bus for every hour of spring season before and after planning. As can be seen, there is a notable enhancement in the overall distribution of voltage. Furthermore, as a consequence of using the chance-constrained programming method, only a minuscule probability of violation occurs at the tail regions of PDFs.

To prove the efficiency and accuracy of the proposed PEM scheme in solving the understudy problem, the MCS with 100,000 scenarios is

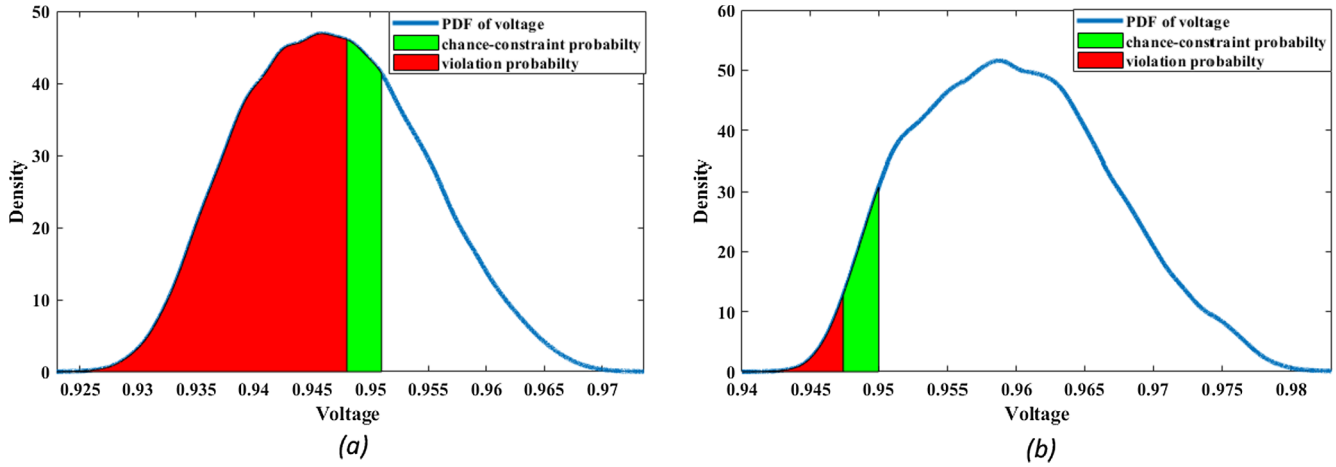

Fig. 10. PDF of voltage at node 15 and hour22 of spring (a) deterministic planning case (b) probabilistic case.

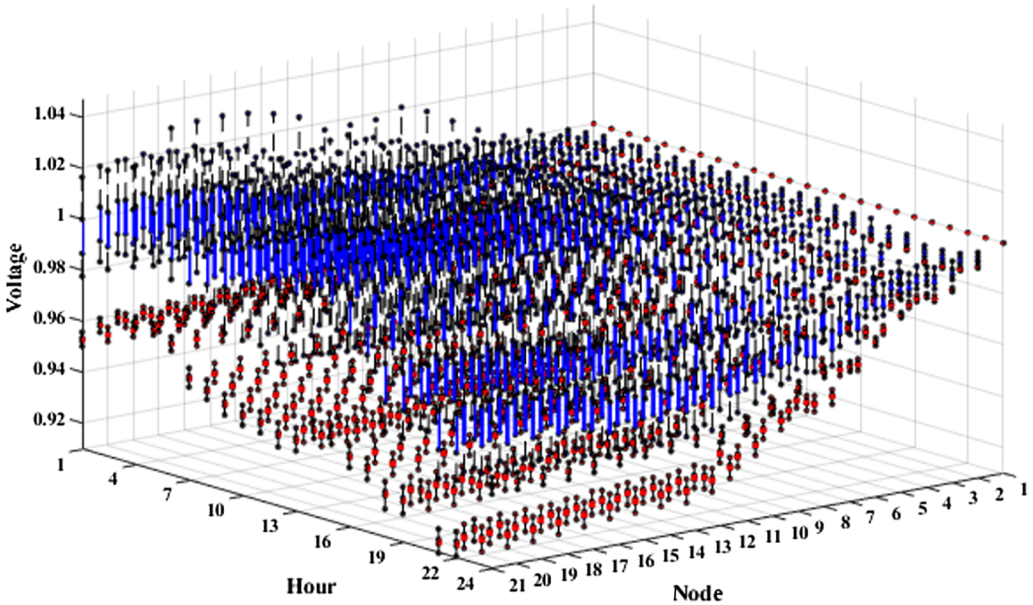

Fig. 11. Voltage distribution at each node and time for spring before planning (red boxplots) and after planning (blue boxplots). (For interpretation of the references to colour in this figure legend, the reader is referred to the web version of this article.)

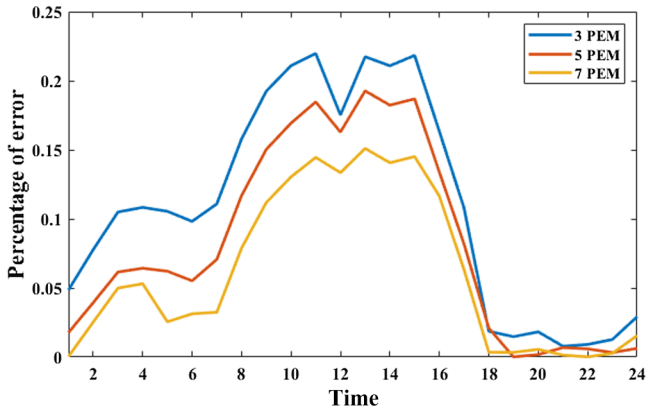

Fig. 12. Percentage of error in the calculation the mean value of the objective function for different PEM schemes.

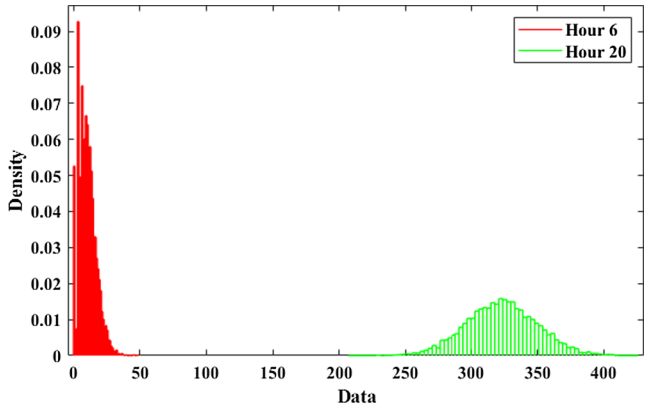

Fig. 13. PEVs' load demand distribution at hour 6 and hour 20.

considered as the accurate reference, and the percentage of error is extracted for three-point, five-point, and seven-point schemes. The results are plotted in Fig. 12. As can be seen, the results with an acceptably low amount of error are obtained within considerably low evaluations, which proves the computational efficiency of the PEM.

Since the violin plot concept as shown in Fig. 2 does not provide all the information about PDFs, the PDF of PEVs power demand at hour 6 and hour 20 of the day is illustrated by Fig. 13. As it is demonstrated, the PDF of PEVs load demand at hour 6 of the day doesn't follow any specific PDF and the data is mostly accumulated around zero. Considering these characteristics, it is impossible to get non-negative estimation points by Hong's PEM. For these particular reasons, it is imperative to use Zhao's PEM in presence of PEVs.

5. Conclusion

In this paper, multi-objective optimal planning of WDGs, SDGs, and CBs is investigated considering different sources of uncertainty, including plug-in electric vehicles. An unconventional PEM is incorporated into the problem to deal with the uncertainties. The results obtained from MCS prove that this method is acceptably accurate, robust, and computationally fast. The asymmetric PDF of PEVs load demand demonstrates the necessity of using a different type of PEM in this particular problem. The analysis of the deterministic and probabilistic case scenarios, reveals that in the deterministic case, the planning components are closer to the end nodes, which have a higher degree of optimality. Whereas, in the probabilistic case, components are distributed along the system. However, the robustness analysis proves that the amount of constraint violation in the probabilistic case is considerably lower than that of the deterministic case. PEVs impose a large uncertain load on the distribution system, which results in lower voltage stability, higher global emissions, and higher cost. However, the proposed multi-objective renewable distributed generation planning provides a reliable solution for this problem. The little probability of violation is the result of using chance-constrained programming and PDF estimation errors, which is insignificantly small. It is also observed that the increments in PEVs penetration level, nonlinearly increases the optimal capacity of the planning components and shifts the Pareto front the less optimal areas of the objective space. As a prospect for future studies, coordinated charging of PEVs in the uncertain environment, the optimal tab position of the transformers, and the islanding mode operation can be integrated into the problem.

CRediT authorship contribution statement

Saeed Zeynali: Conceptualization, Methodology, Software, Validation, Data curation, Formal analysis, Investigation, Writing - original draft. **Naghi Rostami:** Conceptualization, Visualization, Supervision, Project administration, Investigation, Writing - original draft. **M.R Feyzi:** Conceptualization, Visualization, Supervision, Project administration, Investigation, Writing - original draft.

Declaration of Competing Interest

The authors declare that they have no known competing financial interests or personal relationships that could have appeared to influence the work reported in this paper.

Appendix A. Supplementary data

Supplementary data to this article can be found online at https://doi.org/10.1016/j.ijepes.2020.105885.

References

[1] Yang L, Feng B, Li G, Qi J, Zhao D, Mu Y. Optimal distributed generation planning in active distribution networks considering integration of energy storage. Appl Energy 2018;210:1073–81.
[2] Cotia BP, Borges CL, Diniz AL. Optimization of wind power generation to minimize operation costs in the daily scheduling of hydrothermal systems. Int J Electr Power Energy Syst 2019;113:539–48.
[3] Akhbari A, Rahimi M. Control and stability analysis of DFIG wind system at the load following mode in a DC microgrid comprising wind and microturbine sources and constant power loads. Int J Electr Power Energy Syst 2020;117:105622.
[4] Bindeshwar S, Janmejay S. A review on distributed generation planning. Renewable Sustainable Energy Reviews 2017;76:529–44.
[5] Jordehi Rezaee A. Allocation of distributed generation units in electric power systems: a review. Renew Sustain Energy Rev 2016;56:893–905.
[6] Venzke A, Halilbašić L, Barré A, Roald L, Chatzivasileiadis S. Chance-constrained ac optimal power flow integrating hvdc lines and controllability. Int J Electr Power Energy Syst 2020;116:105522.
[7] Ha MP, Huy PD, Ramachandaramurthy VK. A review of the optimal allocation of distributed generation: objectives, constraints, methods, and algorithms. Renew Sustain Energy Rev 2017;75:293–312.
[8] Zhang L, Tang W, Liu Y, Lv T. Multiobjective optimization and decision-making for DG planning considering benefits between distribution company and DGs owner. Int J Electr Power Energy Syst 2015;73:465–74.
[9] Kayal P, Chanda C. Placement of wind and solar based DGs in distribution system for power loss minimization and voltage stability improvement. Int J Electr Power Energy Syst 2013;53:795–809.
[10] Sneha S, Provas Kumar R. Multi-objective quasi-oppositional teaching learning based optimization for optimal location of distributed generator in radial distribution systems. Int J Electrical Power Energy Syst 2014;63:534–45.
[11] El-Fergany and Attia. Optimal allocation of multi-type distributed generators using backtracking search optimization algorithm. Int J Electrical Power Energy Syst 2015;64:1197–205.
[12] Moravej Z, Akhlaghi A. A novel approach based on cuckoo search for DG allocation in distribution network. Int J Electr Power Energy Syst 2013;44(1):672–9.
[13] Liu K-Y, Sheng W, Liu Y, Meng X, Liu Y. Optimal sitting and sizing of DGs in distribution system considering time sequence characteristics of loads and DGs. Int J Electr Power Energy Syst 2015;69:430–40.
[14] Odu G, Charles-Owaba O. Review of multi-criteria optimization methods–theory and applications. IOSR J Eng (IOSRJEN) 2013;3(10):1–14.
[15] Verdejo H, Awerkin A, Kliemann W, Becker C. Modelling uncertainties in electrical power systems with stochastic differential equations. Int J Electr Power Energy Syst

2019;113:322–32.
[16] Soroudi A, Afrasiab M. Binary PSO-based dynamic multi-objective model for distributed generation planning under uncertainty. IET Renew Power Gener 2012;6(2):67–78.
[17] Mokryani G, Siano P. Evaluating the integration of wind power into distribution networks by using Monte Carlo simulation. Int J Electr Power Energy Syst 2013;53:244–55.
[18] Abdelaziz M, Moradzadeh M. Monte-Carlo simulation based multi-objective optimum allocation of renewable distributed generation using OpenCL. Electr Power Syst Res 2019;170:81–91.
[19] Zhang S, Cheng H, Li K, Tai N, Wang D, Li F. Multi-objective distributed generation planning in distribution network considering correlations among uncertainties. Appl Energy 2018;226:743–55.
[20] Zhao Q, Wang S, Wang K, Huang B. Multi-objective optimal allocation of distributed generations under uncertainty based on DS evidence theory and affine arithmetic. Int J Electr Power Energy Syst 2019;112:70–82.
[21] Moradi MH, Abedini M, Tousi SR, Hosseinian SM. Optimal siting and sizing of renewable energy sources and charging stations simultaneously based on Differential Evolution algorithm. Int J Electr Power Energy Syst 2015;73:1015–24.
[22] Liu Z, Wen F, Ledwich G. Optimal siting and sizing of distributed generators in distribution systems considering uncertainties. IEEE Trans Power Delivery 2011;26(4):2541–51.
[23] Ahmadian A, Mahdi S, Aliakbar-Golkar M. Fuzzy load modeling of plug-in electric vehicles for optimal storage and DG planning in active distribution network. IEEE Trans Veh Technol 2017;66(5):3622–31.
[24] Ahmadian A, Mahdi S, Aliakbar-Golkar M. 2015. Stochastic modeling of plug-in electric vehicles load demand in residential grids considering nonlinear battery charge characteristic. In: Electrical Power Distribution Networks Conference (EPDC), 2015 20th Conference on, 2015: IEEE, pp. 22-26.
[25] Santos A., McGuckin N., Nakamoto H.Y., Gray D., Liss S. 2011. Summary of travel trends: 2009 national household travel survey.
[26] Ahmadian A, Mahdi S, Aliakbar-Golkar M, Fowler M, Elkamel A. Two-layer optimization methodology for wind distributed generation planning considering plug-in electric vehicles uncertainty: a flexible active-reactive power approach. Energy Convers Manage 2016;124:231–46.
[27] Hong H. An efficient point estimate method for probabilistic analysis. Reliab Eng Syst Saf 1998;59(3):261–7.
[28] Morales JM, Perez-Ruiz J. Point estimate schemes to solve the probabilistic power flow. IEEE Trans Power Syst 2007;22(4):1594–601.
[29] Verbic G, Canizares CA. Probabilistic optimal power flow in electricity markets based on a two-point estimate method. IEEE Trans Power Syst 2006;21(4):1883–93.
[30] Can C, Wenchuan W, Boming Z, Hongbin S. Correlated probabilistic load flow using a point estimate method with Nataf transformation. Int J Electrical Power 2015;65:325–33.
[31] Zhao Y-G, Ono T. New point estimates for probability moments. J Eng Mech 2000;126(4):433–6.
[32] Mohammadi M, Shayegani A, Adaminejad H. A new approach of point estimate method for probabilistic load flow. Int J Electrical Power Energy Syst 2013;51:54–60.
[33] Williams T, Crawford C. Probabilistic load flow modeling comparing maximum entropy and Gram-Charlier probability density function reconstructions. IEEE Trans Power Syst 2012;28(1):272–80.
[34] Kayal P, Chanda C. Optimal mix of solar and wind distributed generations considering performance improvement of electrical distribution network. Renewable Energy 2015;75:173–86.
[35] HongShuang L, ZhenZhou L, XiuKai Y. Nataf transformation based point estimate method. Chin Sci Bull 2008;53(17):2586.
[36] Eminoglu U., Hocaoglu M. 2007. A voltage stability index for radial distribution networks. In: Universities Power Engineering Conference, 2007. UPEC 2007. 42nd International, 2007: IEEE, pp. 408-413.
[37] Nazir FU, Pal BC, Jabr RA. A Two-Stage Chance Constrained Volt/Var Control Scheme for Active Distribution Networks With Nodal Power Uncertainties. IEEE Trans Power Syst 2019;34(1):314–25.
[38] Duan C, Fang W, Jiang L, Yao L, Liu J. Distributionally robust chance-constrained approximate ac-opf with wasserstein metric. IEEE Trans Power Syst 2018;33(5):4924–36.
[39] Ji L, Niu D, Xu M, Huang G. An optimization model for regional micro-grid system management based on hybrid inexact stochastic-fuzzy chance-constrained programming. Int J Electr Power Energy Syst 2015;64:1025–39.
[40] National Household Travel Survey [Online]. Available: < http://nhts.ornl.gov > ." (accessed).
[41] Zhou A, Qu B-Y, Li H, Zhao S-Z, Suganthan PN, Zhang Q. Multiobjective evolutionary algorithms: a survey of the state of the art. Swarm Evolutionary Computation 2011;1(1):32–49.
[42] Jiang S, Yang S. A strength Pareto evolutionary algorithm based on reference direction for multiobjective and many-objective optimization. IEEE Trans Evol Comput 2017;21(3):329–46.
[43] Coello C.A.C., Brambila S.G., Gamboa J.F., Tapia M.G.C., Gómez R.H. 2019. Evolutionary multiobjective optimization: open research areas and some challenges lying ahead, Complex Intelligent Syst., pp. 1-16, 2019.
[44] Zitzler E., Laumanns M., Thiele L. 2001. SPEA2: Improving the strength Pareto evolutionary algorithm, TIK-report, vol. 103.
[45] Mason K, Duggan J, Howley E. A multi-objective neural network trained with differential evolution for dynamic economic emission dispatch. Int J Electr Power Energy Syst 2018;100:201–21.
[46] Bharothu JN, Sridhar M, Rao RS. Modified adaptive differential evolution based optimal operation and security of AC-DC microgrid systems. Int J Electr Power Energy Syst 2018;103:185–202.
[47] Islam SM, Das S, Ghosh S, Roy S, Suganthan PN. An adaptive differential evolution algorithm with novel mutation and crossover strategies for global numerical optimization. IEEE Trans Syst Man Cybern Part B (Cybern) 2011;42(2):482–500.
[48] Mezura-Montes E., Velázquez-Reyes J., Coello C.C. 2006. Modified differential evolution for constrained optimization. In: Evolutionary Computation, 2006. CEC 2006. IEEE Congress on, 2006: IEEE, pp. 25-32.
[49] Tang L, Wang X. A hybrid multiobjective evolutionary algorithm for multiobjective optimization problems. IEEE Trans Evol Comput 2012;17(1):20–45.
[50] Chamorro HR, Riano I, Gerndt R, Zelinka I, Gonzalez-Longatt F, Sood VK. Synthetic inertia control based on fuzzy adaptive differential evolution. Int J Electr Power Energy Syst 2019;105:803–13.
[51] Rana S., Srivastava R. 2017. Solving Travelling Salesman Problem Using Improved Genetic Algorithm, Indian J Sci Technol, vol. 10, 2017.
[52] Juneja S.S., Saraswat P, Singh K., Sharma J., Majumdar R., Chowdhary S. 2019. Travelling Salesman Problem Optimization Using Genetic Algorithm. In: 2019 Amity International Conference on Artificial Intelligence (AICAI), 2019: IEEE, pp. 264-268.
[53] Eduardo CG, Guimarães FG, Ricardo THC, Neto OM, Felipe C. Electric distribution network expansion under load-evolution uncertainty using an immune system inspired algorithm. IEEE Trans Power Syst 2007;22(2):851–61.
[54] Lotov AV, Miettinen K. Visualizing the Pareto frontier. Multiobjective optimization. Springer; 2008. p. 213–43.
[55] Zio E, Delfanti M, Giorgi L, Olivieri V, Sansavini G. Monte Carlo simulation-based probabilistic assessment of DG penetration in medium voltage distribution networks. Int J Electr Power Energy Syst 2015;64:852–60.
[56] Moradi MH, Abedini M. A combination of genetic algorithm and particle swarm optimization for optimal DG location and sizing in distribution systems. Int J Electr Power Energy Syst 2012;34(1):66–74.
[57] Viral R, Khatod D. An analytical approach for sizing and siting of DGs in balanced radial distribution networks for loss minimization. Int J Electr Power Energy Syst 2015;67:191–201.